



Corrigendum Notice: A corrigendum has been issued for this article and is included at the end of this document.

Article

## Probing molecular architectures and interactions with scanning tunneling microscopy on graphite and arachidic acid functionalized surfaces

 Medet Mustafin\*

Department of Physics and Technology, Al-Farabi Kazakh National University, 71 Al-Farabi ave., Almaty, Kazakhstan

\*Correspondence: [medet.mustafin.01@mail.ru](mailto:medet.mustafin.01@mail.ru)

**Abstract.** This study investigates the application of scanning tunneling microscopy in exploring molecular structures and interfaces relevant to nanotechnology. Graphite was selected as a sample due to its ease of visualization of atomic arrangements and surface inertness. The surface of highly oriented pyrolytic graphite treated with arachidic acid ( $C_{20}H_{32}O_2$ ) was examined to gain insights into the behavior of organic molecules at liquid-solid interfaces. Through detailed observations, the study demonstrates the versatility of scanning tunneling microscopy in elucidating molecular architectures and interactions. The findings underscore the importance of scanning tunneling microscopy in advancing our understanding of molecular systems and driving progress in nanotechnology applications. This work highlights the pivotal role of scanning tunneling microscopy in unraveling the complexities of nanoscale phenomena and fostering future innovations in the field.

**Keywords:** scanning tunneling microscopy, graphite, molecular structures, liquid-solid interfaces, nanotechnology applications

### 1. Introduction

Solid surface atomic composition can be observed with a Scanning Tunneling Microscope (*STM*). These compositions affect the dynamics of the solid, which makes them significant in material physics [1-2]. Quantum tunneling is the foundation of *STM* operation. The quantum mechanical tunneling effect is the fundamental idea that drives *STM* [3-4]. The ability of particles to pass over potential barriers that are taller than their total energy is described by this phenomena. The properties of particle waves are intimately related to the tunneling effect. A model of the energy levels of free electrons in a metal can explain this phenomena [5-6]. The energy of electrons can be expressed by the formula:

$$E = \frac{p^2}{2m} \quad (1)$$

Where,  $p$  is the electron's momentum and  $m$  is its mass, because the electron gas inside the conductor is regarded as free in this model. The Fermi level is the greatest energy an electron can have in a metal at zero temperature [7]. Conduction electrons could potentially find a trench throughout the metal's entire volume. The electrons with the highest energy, or those around Fermi level, are the ones that primarily contribute to the tunnel current. Conduction electrons are located at the edge of the potential well, which acts as a potential barrier for them at the metal surface and the boundary between the metal and vacuum. The output work  $\phi$  determines the height of this potential barrier.

*STM* under ultrahigh vacuum conditions allows obtaining atomic images of the surface of metals and semiconductors, including silicon, by registering the tunneling current between the probe and the surface under study close to it. It is designed to study elementary structural processes on the surface of semiconductors and metals to create nanosystems and new materials with unique

properties. Not only may *STM* be used in ultra-high vacuum, but it can also be employed at temperatures ranging from almost 0 K to more than 1000 °C in air, water, and other liquids or gases with ambient temperatures [8].

Many of the present and future uses of nanotechnology, such as molecular light-harvesting and emitting devices, molecular electronics, biological identification, and molecular sensor technologies, are based on organic molecules [9]. Systems based on molecular thin films are emerging as a very promising path for the near future, whereas single-molecule electronics pose considerable obstacles for practical applications. One prominent technique for developing new molecular architectures is self-assembly, especially when it comes to the production of electrical and optoelectronic devices.

## 2. Methods

In this work, graphite was chosen as a sample for *STM* studies due to the ease of visualization of its atoms and the inertness of its surface. Since each crystallite in synthetic highly oriented pyrolytic graphite (*HOPG*) is perfectly aligned, it is utilized in place of natural graphite. The graphite topographic image presented in Figure 1 has a distinctive hexagonal pattern that is distinct from the honeycomb pattern [10]. This effect is caused by the electrical structure's quirks, which cause only every other atom to be mapped. Because the electron density is focused closer to the bulk, the carbon atoms on the surface, which are positioned above other atoms of the second carbon layer, are not visible [11].

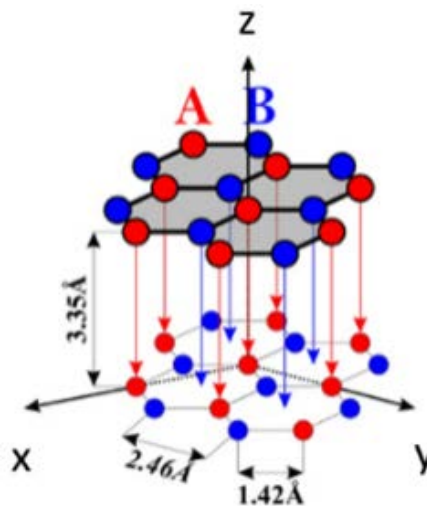


Figure 1 – Graphite's 3D atomic structure

When an electric field is applied to an extremely sharp metal tip in close proximity to an electrically conductive sample, a current flows between the tip and the sample without any physical contact. Using this so-called tunneling current, the electrical topography of the surface of freshly produced graphite is examined on the supplementary nanometer scale. Atoms and hexagonal structures are photographed by scanning the graphite surface line by line with the tip line. Surface topography was investigated using an *STM* operated in ambient air. The *STM* system included vibration isolation and a protective magnetic shield to minimize environmental noise and drift. The scanning head consisted of piezoelectric elements capable of sub-nanometer resolution, enabling precise tip positioning in x, y, and z axes through voltage-controlled expansion [2]. A platinum–iridium metal tip, electrochemically etched to nanometric sharpness, was used throughout the study. The main part of the equipment is scanning, based on a platform for vibration isolation and a protective magnetic cover for tip and sample inspection. Without the necessity for mechanical contact, a current can be produced between a sharp metal tip and an electrically conductive sample when an electric field is introduced. This phenomenon, called tunneling current, is utilized to examine

the surface electron topography of freshly manufactured graphite at an additional nanoscale scale. Atoms and hexagonal structures are photographed through the application of a tip line over the graphite surface. The equipment used in this study was manufactured by Gulmeiy Company.

Figure 2 *a* presents a piezo-elements enable metal tip, which move across a sample's surface during *STM*.

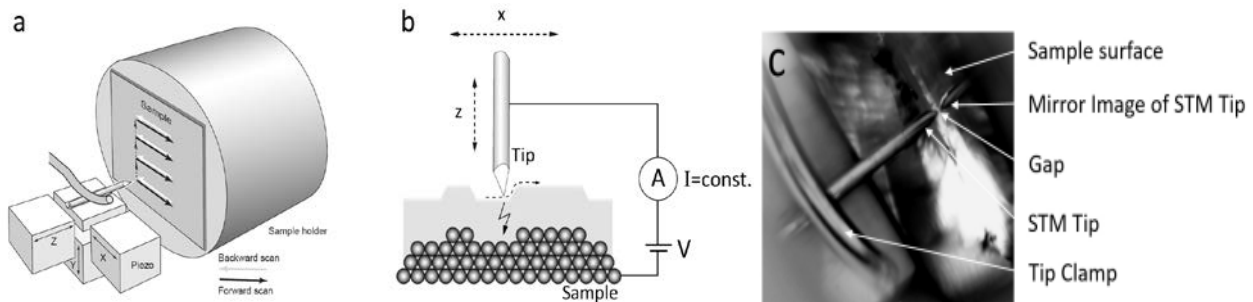


Figure 2 – *STM* sample mounted scheme

In Figure 2 *b* and *c* the tunneling current at which the tip is held is determined by the feedback loop *z*'s operational point. In essence, this establishes the separation between the tip and the model. The tip is nearer the sample surface the higher the set point. 5 nA is typically utilized for graphite atomic resolution.

By varying the voltage, these elements can precisely move the tip at a scale of picometers since they change length in reaction to applied voltage. A tunneling current is created across the tiny gap between the tip and the sample by an applied bias voltage. Constant-current or constant-height modes can be used for surface scanning. The tunneling current in the constant-height mode changes according to the tip's lateral position. The more widely used constant-current mode produces a profile of the sample's height based on the *z*-signal by using a feedback loop to maintain the tip height and keep the tunneling current constant. The tunneling current and distance have an exponential connection (a change of one Angström in distance results in a tenfold change in tunneling current) and the piezo-elements' exact movement allows for an extraordinary resolution, all the way down to the atomic level.

The *P*, *I* and *D* coefficients used in proportional-integral-differential (*PID*) controllers determine how the system reacts to deviations of the measured current from the set point. The number of values that are too low can cause the tip to be insufficiently sensitive to changes in height, while values that are too high can cause tip position fluctuations. Recommended parameter *D* can be set to zero. The values of parameters *P* and *I* was selected based on the current context and system response time. The default value of 1000 is a precise starting value.

The tip voltage indicates the offset applied to the tip. The lower the voltage, the closer the tip is to the surface. The optimum value of the bias voltage depends on the electronic structure of the sample, such as the density of states (*DOS*). For semiconductors, it is important to keep in mind that it is not recommended to place the bias voltage inside the band of forbidden energy states.

The *HOPG* surface was scanned at *STM* in air, which allowed imaging of different sizes, ranging from  $\sim 100$  nm, where step edges are visible, to as small as  $\sim 5$  nm with atomic resolution. The following characteristics of 5 nA, 0.6 nA, 1.3 V have been used for atomic resolution.

For more detailed analysis of a liquid-solid interface, we investigated the surface of *HOPG* treated with arachidic acid  $C_{20}H_{32}O_2$ .

*STM* image acquisition and instrument control were performed using Nanoscope V software (Bruker). Image data were analyzed using Gwyddion 2.63, an open-source software for scanning probe microscopy, which was used for plane correction, noise filtering, and extraction of line profiles.

No statistical testing was required for qualitative imaging results; however, repeated scans were conducted to ensure reproducibility of atomic patterns under identical conditions.

### 3. Results and Discussion

Figure 3 presents the topography surface of the synthetic graphite scanned by *STM*. A scanning probe microscope provides an image of a surface magnified in all three dimensions: *x*, *y* and *z*, with maximum resolution in each axis. *x* –axis have been selected 1.2 nA,  $P_{gain}$  1200,  $I_{gain}$  1500., with the maximum resolution for each axis determined by various factors. The *z*-axis resolution is limited, first, by the sensitivity of the sensor and, second, by the amplitude of the probe vibrations relative to the sample surface. The design of the microscope must be able to reduce the amplitude of these vibrations to fractions of an angstrom.

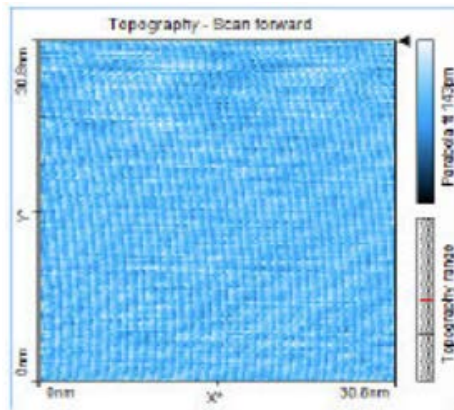


Figure 3 – Topography surface of 30 nm, scanned in 0.14 s, with 1.2 nA,  $P_{gain}$  1200,  $I_{gain}$  1500

Since thermal fluctuations have an impact on nanoscale measurements, we have selected a mode of 0.03 s at 128 "Points/Line" for atomic resolution in order to scan the sample as quickly as possible. Since that four to eight atoms have a diameter of one nanometer, much smaller picture sizes are required to reach atomic resolution. On Figure 4, atomic arrangements are often identifiable at image sizes of roughly 10–3 nm. Consequently: In the imaging panel, set the image size to 3 nm (Figure 5).

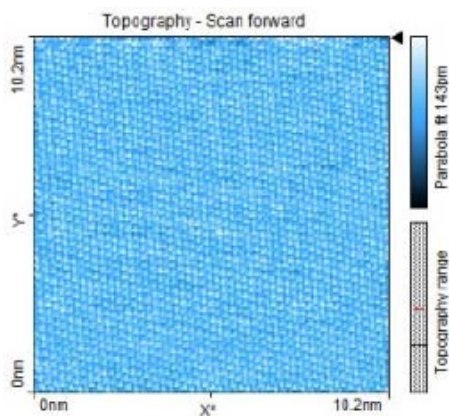


Figure 4 – Topography surface of 10 nm, scanned in 0.03 s, with 1.2 nA,  $P_{gain}$  1200,  $I_{gain}$  1500

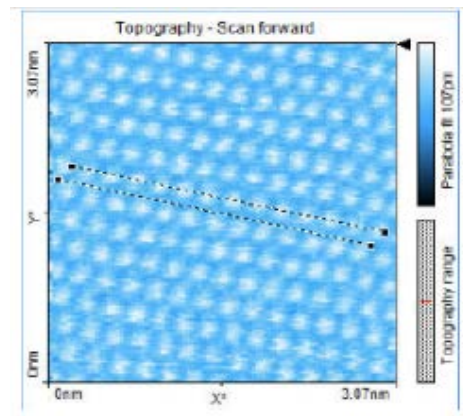


Figure 5 – Topography surface of 3 nm, scanned in 0.03 s, with 1.2 nA,  $P_{gain}$  1300,  $I_{gain}$  850. Line-to-line distance:  $d=138$  pm

To investigate the interface between the liquid-solid interface, we applied arachidic acid  $C_{20}H_{32}O_2$  to the *HOPG*. Figure 6a shows the condition of the test sample applied with arachidic acid. Parameters for scanning were as follows 0.6 nA, 1.3 V, image size  $15.8 \times 15.8$  nm<sup>2</sup>. The scanned image on Figure 6b showed that at fine resolution, the obvious features of arachidic acid, which has

an orange coloration, dominate. However, at the same parameters, it is almost impossible to distinguish individual carbon atoms.

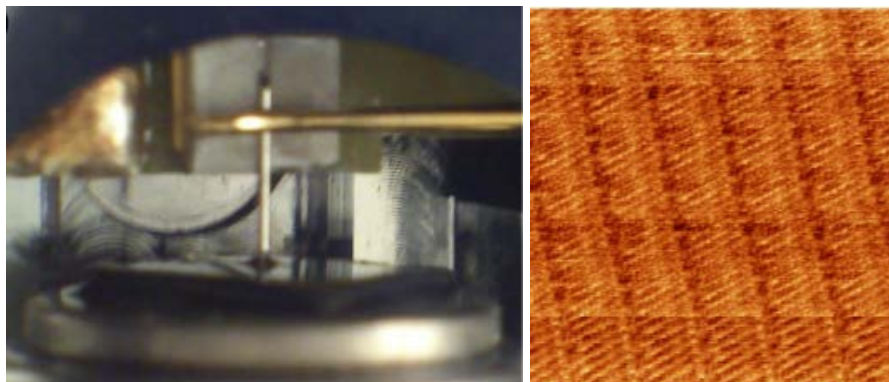


Figure 6 – Applying acid  $C_{20}H_{32}O_2$  on *HOPG* surface: a) test sample; b) scanned image

#### 4. Conclusions

In conclusion, this study demonstrates the versatility and potential of *STM* in investigating various interfaces and molecular structures. By utilizing graphite as a sample, the ease of visualizing atomic arrangements and the inert surface nature facilitated detailed observations. Furthermore, the exploration of the *HOPG* surface treated with arachidic acid provided insights into the behavior of organic molecules at liquid-solid interfaces. These findings underscore the significance of *STM* in advancing our understanding of molecular structures and their interactions, paving the way for further developments in nanotechnology applications, such as molecular electronics, optoelectronic devices, and sensor technologies. Overall, this work highlights the crucial role of *STM* in unraveling the complexities of molecular systems and driving advancements in the field of nanoscience.

#### References

1. Photoelectrochemical cells / M. Grätzel // Nature. — 2001. — Vol. 414, No. 6861. — P. 338–344. <https://doi.org/10.1038/35104607>
2. Surface Characterization of Materials at Ambient Conditions by Scanning Tunneling Microscopy (STM) and Atomic Force Microscopy (AFM) / S.N. Magonov // Applied Spectroscopy Reviews. — 1993. — Vol. 28, No. 1–2. — P. 1–121. <https://doi.org/10.1080/05704929308021499>
3. Scanning Microscopy for Nanotechnology: Techniques and Applications / W. Zhou, Z.L. Wang. — Berlin, Germany: Springer Science & Business Media, 2007. — 533 p.
4. Scanning tunneling microscope study of iron-based superconductors / Q. Zhang, Zh. Xu // Acta Microscopica. — 2019. — Vol. 28, No. 6. — P. 1491–1498.
5. Quantum-correlated fluctuations, phonon-induced bond polarization, enhanced tunneling, and low-energy nuclear reactions in condensed matter / K.P. Sinha, A. Meulenberg // Proceedings of the 16th International Conference on Condensed Matter Nuclear Science, ICCF 2011: "Celebrating the Centenary of the Discovery of the Atomic Nucleus". — 2011. — P. 132–141.
6. High-resolution energy measurement of field-emitted electrons from a single crystalline magnetite whisker / H. Sakakibara, S. Nagai, K. Hata, T. Iwata, M. Okada, H. Mimura // Surface and Interface Analysis. — 2012. — Vol. 44, No. 6. — P. 699–702. <https://doi.org/10.1002/sia.4811>
7. Effects of disorder and temperature on Fermi-energy of one-dimensional disordered systems / Sh. Shang Ma, X. Liu, H. Xu, Y.-F. Li // Journal of Central South University. — 2007. — Vol. 38, No. 2. — P. 281–284 .
8. A low temperature, ultrahigh vacuum, microwave-frequency-compatible scanning tunneling microscope / S.J. Stranick, M.M. Kamna, P.S. Weiss // Review of Scientific Instruments. — 1994. — Vol. 65, No. 10. — P. 3211–3215. <https://doi.org/10.1063/1.1144551>
9. Microtechnology, nanotechnology, and the scanning-probe microscope: an innovative course / J.D. Adams, B.S. Rogers, L.J. Leifer // IEEE Transactions on Education. — 2004. — Vol. 47, No. 1. — C. 51–56. <https://doi.org/10.1109/TE.2003.817623>
10. Topographic modifications on the graphite surface induced by high energy single-ion impact / C.H. de Villeneuve, M. Phaner, L. Porte, N. Monocoffre, P. Pertosa, J. Tousset // Vacuum. — 1990. — Vol. 41, No. 7–9. — P. 1686–1689. [https://doi.org/10.1016/0042-207X\(90\)94055-U](https://doi.org/10.1016/0042-207X(90)94055-U)

11. X-ray topographic determination of the granular structure in a graphite mosaic crystal: A three-dimensional reconstruction / M. Ohler, M. Sanchez Del Rio, A. Tuffanelli, M. Gambaccini, A. Taibi, A. Fantini, G. Pareschi // Journal of Applied Crystallography. — 2000. — Vol. 33, No. 4. — P. 1023–1030. <https://doi.org/10.1107/S0021889800005975>

**Information about author:**

*Medet Mustafin* – Master Student, Department of Physics and Technology, Al-Farabi Kazakh National University, 71 Al-Farabi ave., Almaty, Kazakhstan, [medet.mustafin.01@mail.ru](mailto:medet.mustafin.01@mail.ru)

**Author Contribution:**

*Medet Mustafin* – concept, methodology, resources, data collection, testing, modeling, analysis, visualization, interpretation, drafting, editing, funding acquisition.

**Conflict of Interest:** The authors declare no conflict of interest.

**Use of Artificial Intelligence (AI):** The authors declare that AI was not used.

*Received: 20.11.2023*

*Revised: 02.03.2024*

*Accepted: 11.03.2024*

*Published: 17.04.2024*



**Copyright:** © 2024 by the authors. Licensee Technobius, LLP, Astana, Republic of Kazakhstan. This article is an open access article distributed under the terms and conditions of the Creative Commons Attribution (CC BY-NC 4.0) license (<https://creativecommons.org/licenses/by-nc/4.0/>).



**Corrigendum Notice: A corrigendum has been issued for this article and is included at the end of this document.**

*Post-Publication Notice*

**Corrigendum to “M. Mustafin, “Probing molecular architectures and interactions with scanning tunneling microscopy on graphite and arachidic acid functionalized surfaces”, *tbusphys*, vol. 2, no. 2, p. 0010, Apr. 2025. doi: 10.54355/tbusphys/2.2.2024.0010”**

In the originally published version of this article, the Methods section omitted crucial details about the experimental setup and data acquisition process.

The following corrections have been made:

1. Section 2 (Methods):

- The updated text specifies the STM equipment manufacturer (Gulmev Company), vibration isolation system, feedback loop parameters (PID values), and measurement conditions (bias voltage, tunneling current, scanning speed).

- Additional details on software tools used (Nanoscope V for acquisition, Gwyddion 2.63 for analysis) have been provided.

- The description of repeated scans for reproducibility and imaging conditions for both graphite and arachidic acid-treated surfaces has been expanded.

2. Editorial corrections have been made to clarify technical terminology and improve reproducibility of the experimental methodology.

Additionally, the following references have been updated:

- “Study of superconductors by electron tunneling / I. Giaever, K. Megerle // *Physical Review*. — 1961. — Vol. 122, No. 4. — P. 1101–1111.” has been replaced with “Scanning tunneling microscope study of iron-based superconductors / Q. Zhang, Zh. Xu // *Acta Microscopica*. — 2019. — Vol. 28, No. 6. — P. 1491–1498.”

- “Phonon induced tunneling of ions in solids / J.A. Sussmann // *Physik der Kondensierten Materie*. — 1964. — Vol. 2, No. 2. — P. 146–160.” has been replaced with “Quantum-correlated fluctuations, phonon-induced bond polarization, enhanced tunneling, and low-energy nuclear reactions in condensed matter / K.P. Sinha, A. Meulenberg // *Proceedings of the 16th International Conference on Condensed Matter Nuclear Science, ICCF 2011: "Celebrating the Centenary of the Discovery of the Atomic Nucleus"*. — 2011. — P. 132–141.”

- “Energy distributions of field emitted electrons / R. Stratton // *Physical Review*. — 1964. — Vol. 135, No. 3A. — P. A794–A805.” has been replaced with “High-resolution energy measurement of field-emitted electrons from a single crystalline magnetite whisker / H. Sakakibara, S. Nagai, K. Hata, T. Iwata, M. Okada, H. Mimura // *Surface and Interface Analysis*. — 2012. — Vol. 44, No. 6. — P. 699–702. <https://doi.org/10.1002/sia.4811>.”

These amendments do not affect the results, conclusions, or scientific validity of the article. They enhance transparency and methodological precision.

Published: 15.05.2024



**Copyright:** @ 2024 by the authors. Licensee Technobius, LLP, Astana, Republic of Kazakhstan. This article is an open access article distributed under the terms and conditions of the Creative Commons Attribution (CC BY-NC 4.0) license (<https://creativecommons.org/licenses/by-nc/4.0/>).